Computational Materials Science 55 (2012) 95–99

Contents lists available at SciVerse ScienceDirect

Computational Materials Science

journal homepage: www.elsevier.com/locate/commatsci

# The roles of crosslinks in the buckling behaviors and load transferring mechanisms of double-walled nanotubes under compression

Bei Peng [a,*], Yong Li [a], Shen Liu [b], Zaoyang Guo [c], Li Ding [a]

[a] Department of Mechanical Engineering, University of Electronic Science and Technology of China, Chengdu 611731, PR China
[b] Institute of Mechanics, Chinese Academy of Science, Beijing 100190, PR China
[c] School of Civil Engineering and Geosciences, Newcastle University, Newcastle Upon Tyne NE1 7RU, United Kingdom

ARTICLE INFO

*Article history:*
Received 14 October 2011
Received in revised form 30 November 2011
Accepted 2 December 2011
Available online 12 January 2012

*Keywords:*
Carbon nanotube
Molecular dynamics
Crosslink
Buckling behavior
Load transfer

ABSTRACT

The buckling behaviors as well as the load transfer mechanisms between the shells of double-walled nanotubes (DWNTs) are investigated through a series of molecular dynamics simulations. When buckling occurs, the strain energy of cross-linked (defective) DWNTs undergoes a modest transition indicating that energy gathered in one shell is shared by the other through the inter-shell crosslinks. It is confirmed that the compressive stress applied to the outer shell can be efficiently transferred to the inner shell through the covalent bonds between shells resulting in a uniform load distribution. The existence of inter-shell crosslinks leads to dramatic decreases of the sustainable loads and modest decreases of the Young's modulus. The computational studies imply that the crosslinks can improve the loading conditions and reduce strain energy in carbon nanotubes based nanocomposites and nanoelectromechanical systems.



## 1. Introduction

Carbon nanotubes (CNTs) have received tremendous scientific and industrial interests since discovery [1] due to their exceptional mechanical, electrical, and thermal properties [2,3]. They are proven to be ideal reinforcing constituents in structural composites for a variety of applications from ballistic armors to aerial materials [4–7]. The reinforcing mechanisms of those composites lie in that loads are transferred between CNTs and the polymer matrix through interfacial interactions. However, only the outmost shell participates in the reinforcement because the stress is not able to be effectively transferred to inner shells. In pristine multiwalled nanotubes (MWNTs), adjacent shells are connected by weak van der Waals forces resulting in inter-shell sliding or torsion when loading. To utilize the outstanding mechanical properties of CNTs more effectively the load transfer mechanisms between shells have to be investigated comprehensively.

Experimental works have shown that ion or electron irradiation [8–10] on pristine CNTs improves the mechanical properties of CNTs via covalent-bond-links between adjacent shells. The irradiation induced covalent bonds are significantly stronger than van der Waals interactions, allowing far more efficient load transfer. Recent experimental works conducted by Peng et al. [11] provide direct evidence that electron irradiation of MWNTs leads to improvements in the maximum sustainable loads. When MWNTs are irradiated by a well-controlled exposure of electron with energy of 200 kV, the fracture characteristics change radically resulting in much higher stiffness and load capacity. These enhancements are attributed to the load sharing of shells connected by irradiation-induced cross-linking defects. The irradiation processes are also proven to be efficient to establish inter-tube bridges in CNTs bundles [12–14], which is promising in developing macroscale CNT ropes and fibers.

Molecular dynamics (MD) is widely recognized as a powerful tool to investigate the mechanical behaviors of CNTs under various loading conditions [15–17]. Huhtala et al. [18] performed MD simulations to study the sliding behaviors of double-walled nanotubes (DWNTs) and found that force needed to initiate sliding between the shells of pristine DWNTs is much higher when a covalent cross-link is present. Shen et al. [19] studied the load transfer between the inner and outer shells of MWNTs and found that a few interstitial atoms can improve the stiffness and load transfer efficiently. Peng et al. [11,20] conducted further computational works to complement experimental efforts and demonstrated that irradiation induced crosslinks can be used to tailoring the load carrying capacity of MWNTs by varying the types and densities of defects. Byrne et al. [21,22] showed that the superior mechanical properties of MWNTs can be realized by controlling $sp^3$ inter-wall bonds. Fonseca et al. [23] also showed that inter-wall $sp^3$ bonds and interstitial carbon atoms can efficiently increase load transfer in DWNTs.

Although aforementioned works indicate that inter-tube cross-links play a crucial role in enhancing load transfer between inner

* Corresponding author. Tel.: +86 28 61830598; fax: +86 28 86316540.
*E-mail address:* beipeng@uestc.edu.cn (B. Peng).

0927-0256/$ - see front matter © 2011 Elsevier B.V. All rights reserved.
doi:10.1016/j.commatsci.2011.12.003

and outer shells of MWNTs, most of these results are achieved under tensile loading conditions and there are relatively few studies on the compressive buckling behavior. In this work, series of MD simulations are carried out to investigate the buckling behavior of DWNTs with inter-tube crosslinking defects under uniaxial compression, aiming at understanding the effects of crosslinks on modifying the mechanical properties of DWNTs. The strain energy and morphological changes, together with Young's modulus and critical strains, are examined to evaluate the modifications of DWNTs with varied crosslinking densities. Furthermore, by inspecting the stress variations of the inner tube when load is only applied to the outer tube, the enhancement of load transfer efficiency attributed to the crosslinks is also studied.

## 2. Computational model

The computational model used in this study consists of a section of [5, 5]/[10, 10] DWNTs (Fig. 1a and b), which satisfies the heat of formation stability rule [$n$, $n$] @ [$n+5$, $n+5$] for DWNTs [24]. The system contains 1800 carbon atoms with an initial length of 73.8 Å. After saturating the dangling bonds at both ends of the nanotubes with 60 hydrogen atoms, for the purpose of reducing edge effects [25,26], the length of the tube increases to 75 Å.

The defects presented in CNTs could be either atomic vacancy or Stone–Wales defects [27]. Theoretically, there are three primary types of inter-tube crosslinking defects: the divacancy defect, the interstitial defect, and the nearest neighbor Frenkel pair defect [28]. We use the Frenkel pair defects in our simulation because they show better load transfer performance than the others [20]. Fig. 1c illustrates the structure of a Frenkel pair defect: an atom is displaced into the interstitial region but retains one bond to the outer tube while forming two bonds with the inner tube. In addition, two Frenkel pair defects are added symmetrically on both sides of the axis for its balance.

The adaptive intermolecular reactive bond order (AIREBO) potential [29] is employed in the model which describes the repulsive/attractive pair interaction, the long-range interactions, and bond torional interactions. AIREBO overcomes the limitations of the reactive empirical bond order (REBO) [30] because the latter lacks the long-range dispersion forces and repulsion/attraction terms for non-bonded atoms. Initially, the cutoff distance of long-range interaction is set to be 10.2 Å, and the conjugate gradient (CG) algorithm is applied to minimize the local potential energy. Then the structure is optimized by relaxation at a temperature of 0.1 K for 50 ps to eliminate thermal fluctuations.

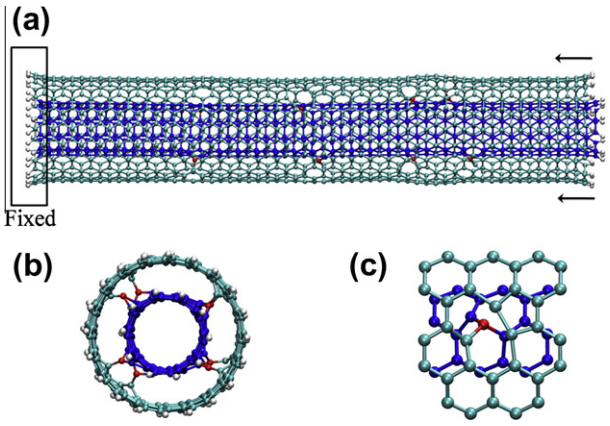


**Fig. 1.** The computational DWNT model with eight Frenkel pair crosslinks after fully relaxation. (a) A top view of the DWNT model. The outer and inner shells are colored cyan and blue, respectively. (b) A cross-sectional view. (c) A detailed view of the crosslinking Frenkel pair defect with the interstitial carbon atoms in red.

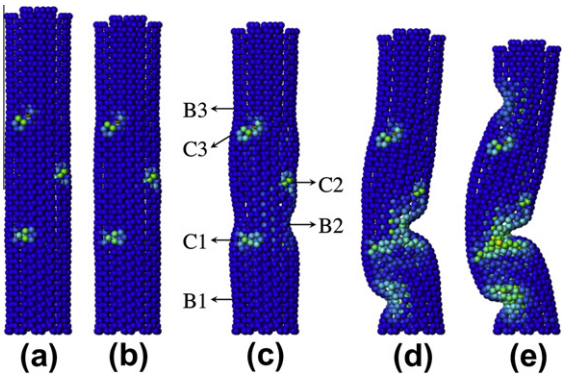


**Fig. 2.** Morphology and strain energy evolution of DWNTs with 6 crosslinks at different strain levels: (a) $\varepsilon = 0$, (b) $\varepsilon = 2.71\%$, (c) buckling point $\varepsilon = 4.54\%$, (d) $\varepsilon = 6.78\%$ and (e) $\varepsilon = 10.00\%$. C1–C3 and B1–B3 in (c) represent the crosslinking numbers and buckling points, respectively.

After the initial relaxation, atoms are held fixed on the left, and a compressive load is applied along the axis of the tube on the right (as shown in Fig. 1a). The loading process is achieved by displacing the atoms left-wards by 0.05 Å each time step, corresponding to ~0.067% of compressive strain. A relaxation process is applied to the system followed by each compression step until the desired strain is achieved. The motions of atoms are governed by the Newtonian equations and are solved by the Velocity-Verlet algorithm [31]. The simulations performed in this work are using the Large-scale Atomic/Molecular Massively Parallel Simulator (LAMMPS) [32], and the atomistic visualizations are created by VMD [33] and Ovito softwares [34].

## 3. Results and discussion

### 3.1. Buckling behaviors

A series of computational work have been carried out by applying compressive strains to both shells of the DWNTs and examining their buckling behaviors. Fig. 2 illustrates the typical deformation procedures of DWNTs with 6 crosslinks at different strain levels. The color which represents the strain energy, a critical parameter describing how external forces distort the tubes, varies from blue[1] (lowest energy) to red (highest energy).

It is obvious that the energy of the crosslinks is much higher than that of the ambient atoms because higher energy is needed to form the crosslinks by shortening or elongating the covalent C–C bonds. Initially the strain energy distributes uniformly along the tube and increases gradually before buckling (Fig. 2a and b). As strain rises, stress starts to accumulate around the crosslinks where an obvious necking is observed at the strain of 4.54% (B2 in Fig. 2c). In all the simulations, buckling (B1–B3) does not exactly take place on a crosslink (C1–C3) but somewhere very close to it, because the energy of the crosslinks is too high to be overcome by the deformation. With continuously increasing of the compressive strain (Fig. 2d and e), the strain energy goes up dramatically around the necking area and spreads to surrounding atoms, resulting in a permanent distortion.

Examining the strain energy helps us to quantitatively analyze the buckling behaviors of DWNTs. Fig. 3 depicts the strain energy as a function of compressive strain for DWNTs with 0, 6 and 12 Frenkel pair crosslinks respectively. In the pre-buckling region (before the transition point), the strain energy increases as a quadratic

[1] For interpretation of color in Figs. 1–7, the reader is referred to the web version of this article.

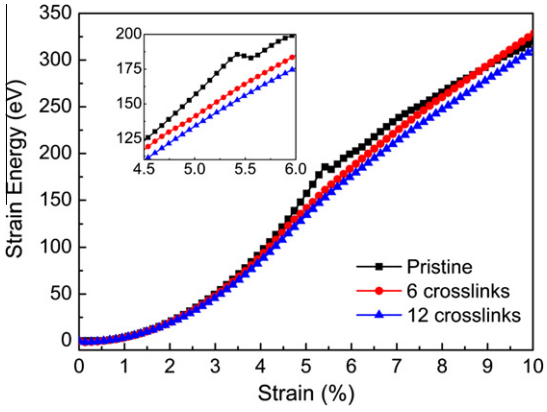


**Fig. 3.** Plot of strain energies as a function of compressive strain for pristine DWNTs and defected DWNTs with 6 and 12 crosslinks. The load is applied on both inner and outer shells. The inserted plot is an enlarged view of the transition region.

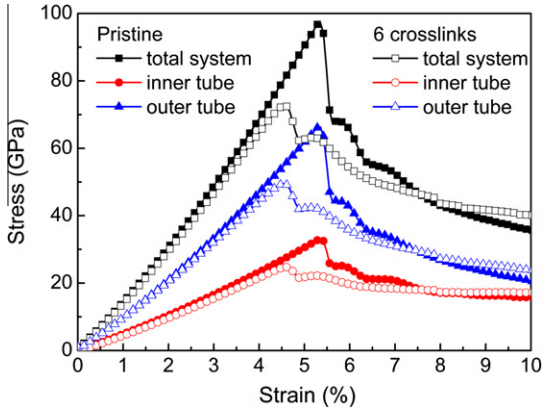


**Fig. 4.** Compressive stress–strain responses of a pristine and a 6-crosslinks DWNTs when both inner and outer tubes are loaded.

function of the compressive strain, i.e. $E \propto \varepsilon^2$, indicating that DWNTs sustain elastic deformations under compressive force. During the post-buckling stage the strain energy increases linearly implying that the system is under constant uniaxial stress [35].

The transition point corresponds to the energy needed for the system to buckle (see the inserted plot of Fig. 3). It is obvious that the transition energy of pristine DWNTs is higher than that of the defective ones. In other words, the presence of crosslinks lowers the threshold energy for DWNTs to buckle. This is because the energy intensified around the crosslinks reaches the critical value even when the total energy of the system is low. Another interesting phenomenon is that the strain energy of pristine nanotubes is subject to a notable decline when buckling, while no apparent change is observed for the defective DWNTs. A possible explanation is that the strain energy gathered in either inner or outer tube can be shared through the inter-shell bridges resulting in a uniform energy distribution (this will be discussed in more details in the load transfer mechanisms part).

The stress–strain curves of the DWNTs with or without crosslinks are plotted in Fig. 4 for comparison. Being consistent with the quadratic behavior of the energy–strain curves (Fig. 3), both pristine and defective DWNTs show elastic deformation until buckling. However, we notice that the buckling stress of the 6-crosslink DWNTs (75.694 GPa) is much lower than that of the pristine ones (101.259 GPa). After the stress reaches its maximum value, a sharp drop of the stress is observed for the pristine nanotubes, while a moderate transition is found for the defective ones. In the post-buckling region, stress of the pristine DWNTs declines more quickly than that of the defective ones do. Fig. 4 also shows even load is applied uniformly to both shells, the outer shell undertakes more stress than the inner shell [17,36]. The Young's modulus, the critical strain and stress for DWNTs with 0, 2, 4, 6, 8, 10 and 12 crosslinks are summarized in Table 1 to understand the effect of defects density on the mechanical properties. The results show that inter-tube crosslinks lead to dramatic decreases in sustainable stress while only modestly decreasing the Young's modulus.

An interesting phenomenon is that the critical stress and Young's modulus does not decrease consistently with the increasing of number of crosslinks. In particular, for the number of crosslinks being 8, it has an unexceptional rise up. The fluctuations are attributed to the asymmetric distribution of crosslinks along axial direction. In the case of odd pairs of crosslinks, i.e. number of crosslinks $N = 2, 6, 10$, the crosslinks are not symmetrically distributed along the axial direction leading to non-uniform stress distribution. However, 8 crosslinks form a more stable and balanced configuration with 4 on each side, leading to rise up of the critical stress and Young's modulus.

### 3.2. Load transfer mechanisms

To further investigate the load/energy transfer mechanisms through inter-tube crosslinks, MD simulations are performed by only loading the outer shell of DWNTs and keeping other parameters the same as previous simulations. Fig. 5 shows the configurations of 12-crosslinked DWNTs at different strains. With compressing of the outer shell, the inner shell deforms too but with a bit of lag (Fig. 5a–d). Fig. 5d shows that the outer shell is compressed by 7.45% while the inner shell only experiences a strain of 2.92%. The strain energy of the crosslinks increases faster than ambient atoms indicating that energy/stress is transferred through them to the inner shell. The buckling behaviors are quite similar with those when both shells are compressed (Fig. 5c and d). Although no external force is applied to the inner shell, it sustains severe structural deformation (Fig. 5e). It is evident that the crosslinks are strong enough to force the inner tube to deform together with the outer tube.

Fig. 6 compares the strain–stress responses of DWNTs with and without crosslinks when only the outer tube is compressed. For the pristine DWNTs, most part of the total stress is applied to the outer tube. The inner tube only sustains a weak stress less than 1 GPa which corresponds to the van der Waals force between shells. With the presence of 12 crosslinks, a portion of the total force is transferred to the inner shell and induces it to buckle. The maximum stress of the inner shell reaches ~8 GPa indicating that the stress applied to the outer shell is effectively transferred to the inner shell.

In order to further investigate the effect of defect density on the efficiency of load transfer, we analyze the induced stress on the

**Table 1**
Calculated Young's modulus, critical strain and stress for DWCNTs with different numbers of Frenkel pair crosslinks under uniaxial compression when both tubes are loaded.

| Number of crosslinks | 0 | 2 | 4 | 6 | 8 | 10 | 12 |
|---|---|---|---|---|---|---|---|
| Critical strain (%) | 5.353 | 4.539 | 4.269 | 4.540 | 4.811 | 4.608 | 4.675 |
| Critical stress (GPa) | 101.259 | 79.115 | 71.598 | 75.694 | 77.926 | 73.320 | 68.056 |
| Young's modulus (Tpa) | 1.678 | 1.634 | 1.617 | 1.607 | 1.625 | 1.595 | 1.542 |

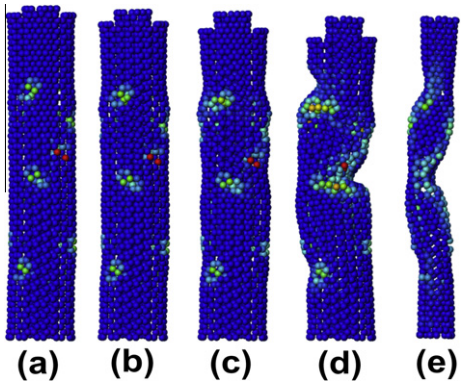


**Fig. 5.** Morphology and strain energy evolution of DWNTs with 12 crosslinks at different strain levels: (a) $\varepsilon = 0$, (b) $\varepsilon = 2.71\%$, (c) buckling point $\varepsilon = 4.94\%$, (d) $\varepsilon = 7.45\%$ and (e) inner tube configuration at $\varepsilon = 7.45\%$.

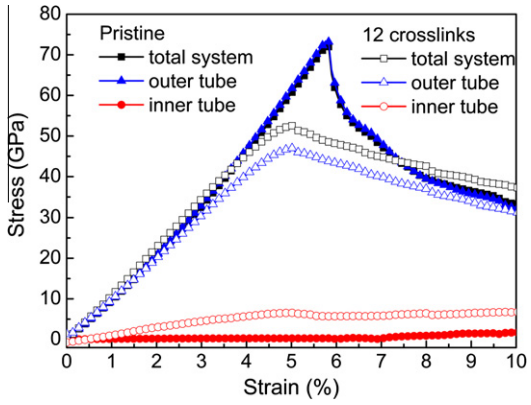


**Fig. 6.** Compressive stress–strain response of pristine and defective DWNTs with 12 crosslinks when only the outer tube is loaded.

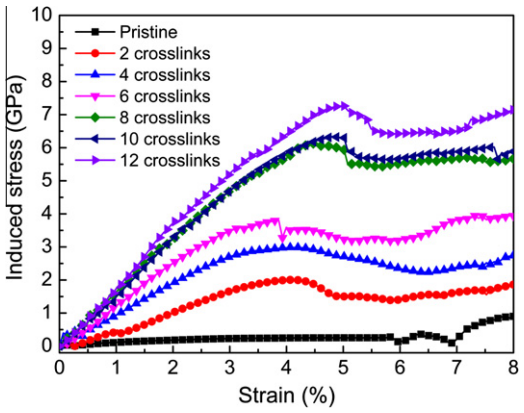


**Fig. 7.** Induced stress vs. strain plot for inner tube of DWNTs with different crosslinks when only the outer tube is loaded.

inner tube as a function of the number of crosslinks (Fig. 7). The stress increases linearly before buckling and fluctuates in the post-buckling stage. The fluctuations are attributed to the reduced inter-shell spacing and the formation of new covalent bonds (Fig. 5d). It is shown clearly that the more crosslinks participate in the more stress is transferred to the inner tube. The results confirm that DWNTs with higher crosslinks density have better load transfer performance.

## 4. Conclusions

The buckling behaviors of pristine and defective DWNTs under uniaxial compressive loads are studied by means of MD simulation, with an emphasis on the load transfer mechanisms of the Frenkel pair crosslinks between adjacent walls. Results show that inter-tube crosslinks reduce the buckling stress of nanotube dramatically while only modestly reduce the Young's modulus. Although introducing of crosslinks sacrifices part of the sustainable strength of the material, it avoids the sharp drop of the stress when buckling and is more stable in the post-buckling stage. The findings in the above investigation give us useful implications in utilizing CNTs based nanocomposites, particularly for materials to resist high speed impact such as ballistic armor.

Further simulations are performed by applying compressive loads to the outer tube only to reveal the load transfer mechanisms and efficiency. Results show that the compressive stress applied to the outer tube can be efficiently transferred to the inner tube through the covalent bonds, which have stronger bonding energy compared to the weak van der Waals force in pristine DWNTs. The computational study also reveals that DWNTs with higher crosslink density have better load transfer performance. The findings in this paper are of particular value in the design and fabricate super strong CNTs reinforced composite and macroscale CNT fibers. The observations illustrate crosslinks play an important role in transferring load/energy between shells which has potential applications in MWNTs, multi-layer graphene sheets and high-strength CNT fibers [13,21,37].

## Acknowledgments

The authors acknowledge the supporting from the National Natural Science Foundation of China Nos. 50801009 and 91123023, the Fundamental Research Funds for the Central Universities No. E022050205. We would like to express our appreciation to H.Z. Huang for supporting this work.

## References

[1] S. Iijima, Nature 354 (1991) 56–58.
[2] R.S. Ruoff, D.C. Lorents, Carbon 33 (1995) 925–930.
[3] S.J. Tans, A.R.M. Verschueren, C. Dekker, Nature 393 (1998) 49–52.
[4] M. Cadek, J.N. Coleman, V. Barron, K. Hedicke, W.J. Blau, Appl. Phys. Lett. 81 (2002) 5123–5125.
[5] A.H. Barber, S.R. Cohen, H.D. Wagner, Appl. Phys. Lett. 82 (2003) 4140–4142.
[6] J.J. Qiu, C. Zhang, B. Wang, R. Liang, Nanotechnology 18 (2007) 275708.
[7] F. Pavia, W.A. Curtin, Acta Mater. 59 (2011) 6700–6709.
[8] A.V. Krasheninnikov, K. Nordlund, J. Keinonen, F. Banhart, Phys. Rev. B 66 (2002) 245403.
[9] A.V. Krasheninnikov, F. Banhart, Nat. Mater. 6 (2007) 723–733.
[10] O. Lehtinen, T. Nikitin, A.V. Krasheninnikov, L.T. Sun, F. Banhart, L. Khriachtchev, J. Keinonen, New J. Phys. 13 (2011) 073004.
[11] B. Peng, M. Locascio, P. Zapol, S. Li, S.L. Mielke, G.C. Schatz, H.D. Espinosa, Nat. Nanotechnol. 3 (2008) 626–631.
[12] A. Kis, G. Csanyi, J.P. Salvetat, T.N. Lee, E. Couteau, A.J. Kulik, W. Benoit, J. Brugger, L. Forro, Nat. Mater. 3 (2004) 153–157.
[13] C.F. Cornwell, C.R. Welch, J. Chem. Phys. 134 (2011) 204708.
[14] T. Filleter, R. Bernal, S. Li, H.D. Espinosa, Adv. Mater. 23 (2011) 2855–2860.
[15] K.M. Liew, C.H. Wong, M.J. Tan, Acta Mater. 54 (2006) 225–231.
[16] Y.Y. Zhang, C.M. Wang, V.B.C. Tan, Nanotechnology 20 (2009) 215702.
[17] C.H. Wong, Comput. Mater. Sci. 49 (2010) 143–147.
[18] M. Huhtala, A.V. Krasheninnikov, J. Aittoniemi, S.J. Stuart, K. Nordlund, K. Kaski, Phys. Rev. B 70 (2004) 045404.
[19] G.A. Shen, S. Namilae, N. Chandra, Mater. Sci. Eng. A 429 (2006) 66–73.
[20] M. Locascio, B. Peng, P. Zapol, Y. Zhu, S. Li, T. Belytschko, H.D. Espinosa, Exp. Mech. 49 (2009) 169–182.
[21] E.M. Byrne, M.A. McCarthy, Z. Xia, W.A. Curtin, Phys. Rev. Lett. 103 (2009) 045502.
[22] E.M. Byrne, A. Letertre, M.A. McCarthy, W.A. Curtin, Z. Xia, Acta Mater. 58 (2010) 6324–6333.
[23] A.F. Fonseca, T. Borders, R.H. Baughman, K.J. Cho, Phys. Rev. B 81 (2010) 045429.
[24] B. Shan, K. Cho, Phys. Rev. B 73 (2006) 081401.
[25] G.E. Froudakis, Nano Lett. 1 (2001) 179–182.

[26] C.Y. Zhi, X.D. Bai, E.G. Wang, Appl. Phys. Lett. 81 (2002) 1690–1692.
[27] H.J. Choi, J. Ihm, S.G. Louie, M.L. Cohen, Phys. Rev. Lett. 84 (2000) 2917–2920.
[28] R.H. Telling, C.P. Ewels, A.A. El-Barbary, M.I. Heggie, Nat. Mater. 2 (2003) 333–337.
[29] S.J. Stuart, A.B. Tutein, J.A. Harrison, J. Chem. Phys. 112 (2000) 6472–6486.
[30] D.W. Brenner, Phys. Status Solidi B 217 (2000) 23–40.
[31] W.C. Swope, H.C. Andersen, P.H. Berens, K.R. Wilson, J. Chem. Phys. 76 (1982) 637–649.
[32] S. Plimpton, J. Comput. Phys. 117 (1995) 1–19.
[33] W. Humphrey, A. Dalke, K. Schulten, J. Mol. Graphics 14 (1996) 33–38 (27–38).
[34] S. Alexander, Modell. Simul. Mater. Sci. Eng. 18 (2010) 015012.
[35] J. Feliciano, C. Tang, Y.Y. Zhang, C.F. Chen, J. Appl. Phys. 109 (2011) 084323.
[36] D.D. Kulathunga, K.K. Ang, J.N. Reddy, J. Phys.: Condens. Matter 22 (2010) 345301.
[37] Y.Y. Zhang, C.M. Wang, Y. Cheng, Y. Xiang, Carbon 49 (2011) 4511–4517.